



Green  
Chemistry

**Kinetics and Mechanism for Hydrothermal Conversion of Polyhydroxybutyrate (PHB) for Wastewater Valorization**

Journal:	<i>Green Chemistry</i>
Manuscript ID	GC-ART-07-2019-002507.R1
Article Type:	Paper
Date Submitted by the Author:	05-Sep-2019
Complete List of Authors:	Li, Yalin; University of Illinois at Urbana-Champaign, Institute for Sustainability, Energy, and Environment Strathmann, Timothy; Colorado School of Mines, Department of Civil and Environmental Engineering; National Renewable Energy Laboratory, National Bioenergy Center

SCHOLARONE™  
Manuscripts

1           Kinetics and Mechanism for Hydrothermal Conversion of  
2           Polyhydroxybutyrate (PHB) for Wastewater Valorization

3                                   Yalin Li<sup>a,b,†</sup> and Timothy J. Strathmann<sup>a,b,c,\*</sup>

4   <sup>a</sup> Department of Civil and Environmental Engineering, Colorado School of Mines, Golden,  
5   Colorado 80401, USA

6   <sup>b</sup> Engineering Research Center for Re-inventing the Nation's Urban Water Infrastructure  
7   (ReNUWIt), Colorado School of Mines, Golden, Colorado 80401, USA

8   <sup>c</sup> National Bioenergy Center, National Renewable Energy Laboratory, Golden, Colorado 80401,  
9   USA

10   <sup>†</sup> Present Address: Institute for Sustainability, Energy, and Environment, University of Illinois at  
11   Urbana-Champaign, Urbana, IL 61801, USA

12   \* Corresponding Author: T. J. Strathmann, E-mail: strthmnn@mines.edu, Phone: +1 (303) 384-  
13   2226

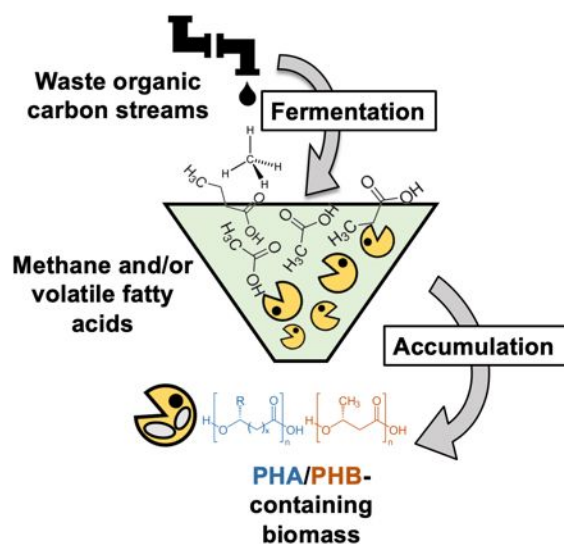
**14 Abstract**

15 Conventional wastewater treatment processes can be tailored to recover organic carbon from  
16 wastewater as intracellular polyhydroxybutyrate (PHB) polymer granules while simultaneously  
17 meeting effluent discharge standards. Traditional applications of PHB as a bioplastic are hampered  
18 by its suboptimal properties (e.g., brittle), lack of efficient and sustainable approaches for  
19 recovering PHB from cells, and concerns about wastewater-derived impurities. In this study, we  
20 report on the conversion of PHB and its monomer acids – 3-hydroxybutyric acid (3HBA) and  
21 crotonic acid (CA) – under hydrothermal conditions (in condensed water at elevated temperature  
22 and pressure) to form propylene, a valuable chemical intermediate that self-separates from water.  
23 PHB depolymerization results in a mixture of 3HBA and CA, which can interconvert via  
24 (de)hydration reactions that vary with prevailing reaction conditions. Further hydrothermal  
25 conversion of the monomer acids yields propylene and CO<sub>2</sub>. Conversion of 3HBA occurs at lower  
26 temperatures than CA, and a new concerted dehydration-decarboxylation pathway is proposed,  
27 which differs from the sequential dehydration (3HBA to CA) and decarboxylation (CA to  
28 propylene and CO<sub>2</sub>) pathway reported for dry thermal conversion. A kinetics network model  
29 informed by experimental results reveals that CA conversion to propylene and CO<sub>2</sub> proceeds  
30 predominantly via hydration to 3HBA followed by the concerted dehydration-decarboxylation  
31 pathway rather than by direct decarboxylation of CA. Demonstrative experiments using PHB-  
32 containing methanotrophic biomass show results consistent with the model, producing propylene  
33 at near-theoretical yields at lower temperatures than reported previously.

## 34 1. Introduction

35 Sustainable management of wastewater represents a major challenge for public utilities, in part,  
36 due to inefficiencies of the existing infrastructure. Most notably, conventional wastewater  
37 treatment facilities employ a combination of energy- and chemical-consuming processes to remove  
38 organic matters and excess nutrients. For example, energy intensive aeration processes are used to  
39 oxidize organic carbon to CO<sub>2</sub>.<sup>1,2</sup> To address these challenges and flip the energy balance of  
40 wastewater treatment operations, alternative processes that can treat wastewater while  
41 simultaneously recovering valuable resources from the waste stream (e.g., fuels and other valuable  
42 chemicals) are attracting growing attention.<sup>3-5</sup> Recent reports demonstrate that organic carbon in  
43 wastewater can be recovered and valorized as intracellular polyhydroxyalkanoate (PHA)  
44 biopolymer granules,<sup>6-8</sup> in particular polyhydroxybutyrate (PHB, PHA with C<sub>4</sub> monomers, **Figure**  
45 **1**).<sup>9-11</sup> For example, waste organic matters can be converted to volatile fatty acids through  
46 acidogenic fermentation, which can then be used to select PHA/PHB-accumulating bacteria and  
47 enrich their PHA/PHB contents;<sup>6,7,12,13</sup> alternatively, biogas generated from anaerobic digestion  
48 can be leveraged for PHB production by methanotrophic bacteria.<sup>14-16</sup> Both of these approaches  
49 have been demonstrated at pilot scale,<sup>6,7,16</sup> and harvested biomass from these processes have been  
50 shown to accumulate up to 50–90% PHA/PHB content on cell dry weight basis.<sup>8,17,18</sup> To date, most  
51 of the efforts have been limited to utilizing PHB as a bio-derived and biodegradable alternative to  
52 petroleum-derived plastics,<sup>19-21</sup> which requires PHB to be separated from the biomass and purified  
53 to high grade. Separation of PHB often involves toxic halogenated solvents (e.g., chloroform,  
54 dichloromethane) for high recovery and purity,<sup>22</sup> though use of green solvents (e.g., methanol,  
55 propanol, acetic acid)<sup>23</sup> has been studied, their use at industrial scales can be very costly.<sup>24</sup> Other  
56 approaches including chemical/biological digestion, supercritical fluids extraction, and

57 mechanical disruption have been explored, but these methods may lead to poor recovery or  
 58 degradation of PHB, or they can be of high cost due to the multiple steps involved.<sup>24</sup> Further, the  
 59 high cost of pure substrates (e.g., glucose, glycerol)<sup>25</sup> for bio-synthesis of PHB diminishes the  
 60 economic viability, and use of waste substrates is limited by concerns about carryover of impurities  
 61 and toxic contaminants. Additionally, the brittle nature, low thermal stability, and weak durability  
 62 of PHB also limit its practical use as a plastic substitute.<sup>26,27</sup>



63  
 64 **Figure 1.** Production of PHA (blue)/PHB (red) biopolymers from waste organic carbon streams.

65 Alternatively, recent efforts reveal that intracellular PHB granules can be converted to  
 66 propylene – a valuable industrial chemical intermediate – when PHB-containing biomass is  
 67 subjected to hydrothermal conditions (i.e., in condensed water at elevated temperature and  
 68 pressure).<sup>28,29</sup> Hydrothermal technologies are well-suited to process wet solids (80–90% moisture  
 69 level) as they require much less energy for feedstock dewatering than complete drying needed by  
 70 processes like pyrolysis. By leveraging the unique properties of water under hydrothermal  
 71 conditions (e.g., increased ion product promoting hydrolysis reactions, decreased dielectric  
 72 constant leading to higher solubility of organic compounds<sup>30,31</sup>), PHB in the biomass can be

73 converted to propylene that self-separates from the aqueous phase,<sup>28,29</sup> creating opportunities for  
74 efficient utilization of PHB and non-PHB cellular materials (NPCMs) that can be simultaneously  
75 converted to biocrudes and upgraded to hydrocarbon fuels.<sup>32</sup> Despite the relative high temperature  
76 and pressure (up to 350°C and 30 MPa) involved in subcritical hydrothermal technologies,<sup>31</sup>  
77 existing studies on its application for algal biofuels indicate that the process can have overall  
78 beneficial impacts on the environment,<sup>33,34</sup> and the process can be economically competitive when  
79 low-cost waste-derived biomass feedstocks are used.<sup>35,36</sup> While previous studies observed  
80 propylene as a co-product of the biocrude oil formed during hydrothermal liquefaction (HTL) of  
81 PHB-containing biomass,<sup>28,29</sup> little is known about the controlling mechanism and process kinetics.  
82 Existing reports of PHB conversion have been limited mostly to pyrolysis (i.e., pure PHB heated  
83 in absence of water or oxygen, also known as thermal decomposition),<sup>37-40</sup> and available reports<sup>41</sup>  
84 on PHB fate under hydrothermal conditions have focused on depolymerization reactions while  
85 further reactions of the resulting monomer acids – 3-hydroxybutyric acid (3HBA) and crotonic  
86 acid (CA) – have been largely ignored. The limited understanding of reaction kinetics and  
87 mechanism creates critical gaps in applying hydrothermal technologies for valorization of PHB-  
88 containing biomass, and should be addressed to evaluate the potential of such approaches for  
89 resource recovery from waste organic streams.

90 The objective of this work was to study the kinetics and mechanism of PHB conversion under  
91 hydrothermal conditions. Depolymerization of PHB and dehydration and decarboxylation of  
92 generated monomers 3HBA and CA were conducted at varying reaction temperatures (175–300°C)  
93 with different initial reactant loadings (0.1–1M) and amendments (acid, base, and salts of  
94 carboxylic acids). A new concerted dehydration-decarboxylation (DHYD-DCXY) mechanism  
95 was proposed for 3HBA and a reaction network was established with kinetics data used for

96 deriving Arrhenius parameters for decomposition of 3HBA and CA. Conversion of PHB-  
97 containing biomass was demonstrated at milder conditions than previously reported and confirmed  
98 the identified mechanisms. Findings from this study provide important insights on hydrothermal  
99 conversion of biomass enriched in PHB and other polyhydroxyalkanoates (PHAs), thereby  
100 advancing a promising new strategy for enhanced valorization of organic components in  
101 wastewater.

## 102 **2. Experimental**

### 103 **2.1. Depolymerization of model polyhydroxybutyrate (PHB)**

104 Depolymerization of commercially sourced PHB (Sigma-Aldrich, natural origin in powder  
105 form) was conducted in stainless steel tube reactors (3/8" outer diameter × 3" length, 0.049" wall  
106 thickness). Details on reactor construction are provided in the Electronic Supplementary  
107 Information (ESI, Section S1, Figure S1). For each experiment, the desired mass (17.2–172.2 mg)  
108 of PHB was added to the reactor with 2 mL of aqueous solution (deionized water with or without  
109 amendments). The reactor was then sealed and immersed in a fluidized sand bath (Accurate  
110 Thermal Systems, FTBLL12) for desired reaction time, after which time the reactor was immersed  
111 in room-temperature water to rapidly terminate reactions. Autogenous pressure was maintained  
112 during the reaction (the maximum pressure was estimated to be around 2.3 MPa for 220°C from  
113 saturated steam tables<sup>42</sup>) and was not expected to have major effects on the reaction.<sup>43,44</sup>  
114 Temperature-time profiles were measured with a thermocouple inserted inside a reactor containing  
115 2 mL of water (Figure S2 in the ESI). These measurements showed that <3 min was required to  
116 heat the reactor to the setpoint temperature or cool the reactor back to room temperature. After  
117 cooling, the reactor was opened and liquid contents were poured into a syringe attached with a  
118 0.45 µm filter (cellulose acetate, Whatman®). The filtrate was then analyzed for monomer acids

119 of PHB (3-hydroxybutyric acid, 3HBA and crotonic acid, CA). The reactor and syringe filter were  
120 dried at 65°C before weighing, and the mass difference before and after reaction were used to  
121 estimate the quantity of residual PHB solids. A wide range of reaction conditions, including  
122 temperature (175, 200, 205, 210, 215, and 220°C), initial PHB loading (0.1, 0.25, 0.5, 0.75, and 1  
123 M as monomers), and various amendments (3HBA, CA, H<sub>2</sub>SO<sub>4</sub>, NaOH, and sodium salts of 3HBA,  
124 CA, butyric acid, and formic acid) were evaluated. All experiments were conducted at least in  
125 duplicate. Details on product analyses are provided in Section S2 in the ESI.

## 126 **2.2. Conversion of PHB monomer acids to propylene**

127 For experiments conducted using PHB monomer acids as starting materials, reactions were  
128 conducted in tube reactors sealed on one end with a bleed valve to enable gas sampling after  
129 quenching reactions (Figure S1 in the ESI). For each experiment, 2 mL of aqueous solution  
130 prepared from the desired PHB-derived monomer acid was added to the reactor, which was then  
131 heated in the fluidized sand bath and quenched in the same manner described for depolymerization  
132 reactions. The maximum autogenous pressure was estimated to be around 8.6 MPa for 300°C from  
133 saturated steam tables<sup>42</sup> and was not expected to have major effects on the reaction.<sup>43,44</sup> After  
134 cooling, the bleed valve was opened to collect headspace gas in a sampling bag (0.5 L ALTEF,  
135 Restek) for subsequent analysis. Gas product composition was analyzed for N<sub>2</sub>, O<sub>2</sub>, CO, CO<sub>2</sub>,  
136 propylene and other volatile (C<sub>1</sub>–C<sub>6</sub>) hydrocarbons (analytical details provided in Section S2 of  
137 the ESI). Aqueous contents of the reactor were then collected and analyzed following the same  
138 procedures described for depolymerization reactions. Effects of temperature (200–275°C for  
139 3HBA and 225–300°C for CA with 25°C interval) and initial reactant loading (0.25, 0.5, and 0.75  
140 M) were investigated. Kinetics data were typically collected at time 0.5, 1, 2, and 4 h, but sampling  
141 time for some reactions was adjusted to accommodate higher reaction rates.



### 142 **2.3. Kinetics modeling**

143 Reaction kinetics data collected from conversion of 3HBA and CA were modeled as a network  
144 of reactions following (pseudo-) first-order rate law, and a least-squares objective function (to  
145 minimize the sum of squared errors between experimental results and model predictions)<sup>45</sup> was  
146 used to calculate rate constants for individual reactions within the network model. Rate constants  
147 determined at varying temperatures were then used to estimate apparent activation energies ( $E_a$ ,  
148  $\text{kJ}\cdot\text{mol}^{-1}$ ) and pre-exponential factors ( $A$ ) according to the Arrhenius Equation:

$$149 \quad \ln k_{\text{obs}} = -\frac{E_a}{RT} + \ln A \quad (\text{Eq. 1})$$

150 The Arrhenius parameters for each reaction in the network model were then applied to numerically  
151 calculate concentration timecourse profiles of each species to compare with experimental results  
152 for internal model validation.

### 153 **2.4. Hydrothermal conversion of PHB-containing biomass**

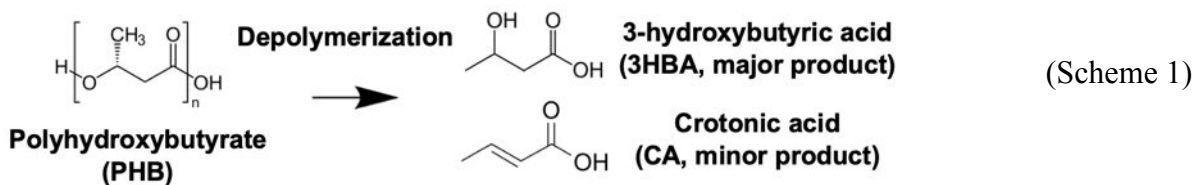
154 Demonstrative experiments were conducted using PHB-containing biomass relevant to  
155 wastewater treatment operations. The biomass was provided by Mango Materials (Albany, CA,  
156 USA) and was dried in an oven at 70°C overnight and ground before analysis or use in experiments.  
157 PHB content of the biomass was measured by the supplier via acid methanolysis followed by gas  
158 chromatography analysis, C/H/N contents were measured by Huffman Hazen Laboratories  
159 (Golden, CO, USA), O content was estimated by difference ( $1 - \text{C}\% - \text{H}\% - \text{N}\%$ ), and ash content was  
160 measured by calcination at 550°C. Hydrothermal conversion of the biomass was conducted in the  
161 same reactors used for conversion of acid monomers. For each reaction, 86.1 mg of the biomass  
162 was mixed with 2 mL aqueous solution before sealing the reactor. The reactor was then heated to  
163 the designated temperature (250, 275, and 350°C) and time (1–6 h depending on temperature)  
164 before quenching. Quantification and analyses of products followed the same protocols described

165 above. Additional experiments were conducted at 250°C for 4 h with H<sub>2</sub>SO<sub>4</sub> as the amendment. A  
 166 control experiment was conducted with PHB-containing biomass replaced by commercially  
 167 sourced PHB to probe potential interactions between PHB and NPCMs in the biomass.

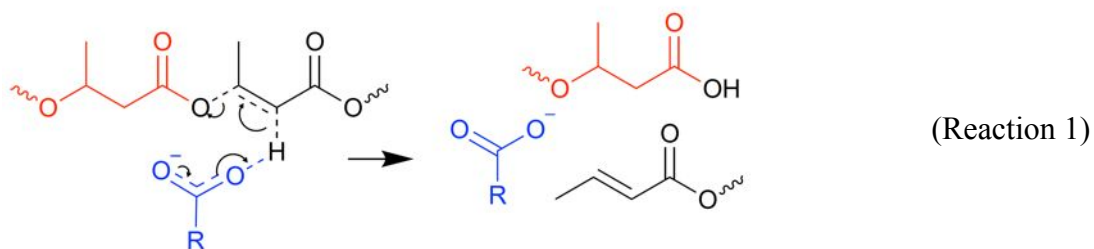
### 168 3. Results and discussion

#### 169 3.1. Depolymerization of PHB

170 Hydrothermal reaction of PHB granules was first examined at mild conditions (175–220°C) to  
 171 provide insights into factors controlling depolymerization (**Table 1**). Minimal depolymerization  
 172 was observed for reaction at 175°C for 2 h, but a mixture of dissolved oligomers and monomers  
 173 3HBA and CA were observed when temperatures were increased to 200°C. When temperature was  
 174 further increased, more 3HBA and CA were generated with a concurrent reduction in residual PHB  
 175 solid and oligomers, and almost no PHB remained after 2 h when temperature was ≥215°C. Further,  
 176 higher temperatures led to decreased carbon recovery (78.1±1.1% at 220°C vs. 91.9±3.5%  
 177 recovery for all reactions at 200°C with varying PHB loading and amendments), which was  
 178 expected to be a result of generated 3HBA and CA decomposing into gas products (discussed in  
 179 **Section 3.2**). The selectivity of monomer acids favored 3HBA at all temperatures ([3HBA]:[CA]  
 180 around 2.1–3.1; Scheme 1). In addition, the initial PHB concentration (0.1–1 M) was found to have  
 181 minimal effect on both the extent of depolymerization and selectivity of monomer products (40–  
 182 50% of PHB conversion after 2 h at 200°C, 3HBA as the major product).

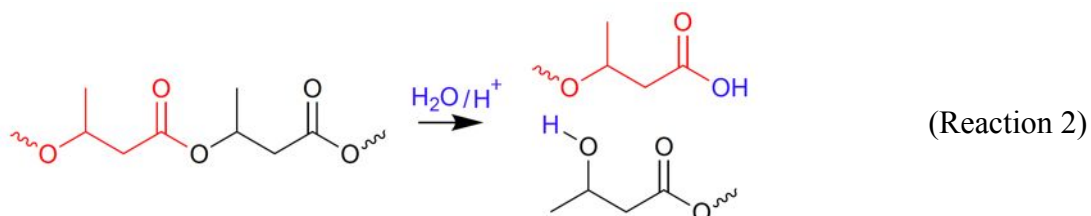


183 In contrast, changes in the aqueous media composition did significantly influence both the rate  
184 of PHB depolymerization and the resulting selectivity of monomer acids. Amending the initial  
185 reaction solution with either monomer acid (3HBA or CA, 0.5 M) catalyzed PHB  
186 depolymerization, with the latter exerting a more pronounced effect (PHB depolymerization after  
187 2 h increased from  $44.7 \pm 2.9\%$  to  $87.2 \pm 1.6\%$  when CA was added vs.  $65.5 \pm 0.7\%$  when 3HBA was  
188 added). While addition of monomer acids lowered the initial pH of the solution (pH measurements  
189 were 2.33 and 2.47 for 0.5 M 3HBA and CA, respectively), acidification of the PHB mixture to  
190 the same pH range using  $\text{H}_2\text{SO}_4$  had a much smaller effect on depolymerization, indicating that  
191 the monomer acids catalyzed PHB depolymerization via a mechanism other than increasing  $\text{H}^+$   
192 concentration. This conclusion was further supported by experiments showing near-complete  
193 depolymerization of PHB in solutions amended with 0.5 M 3HBA and CA that were neutralized  
194 to pH 7 before initiating the reaction. PHB depolymerization was also catalyzed in neutral-pH  
195 solutions amended with formate or butyrate salts ( $99.4 \pm 0.6\%$  and  $74.8 \pm 7.3\%$  depolymerization  
196 after 2 h, respectively). Collectively, these findings indicate that the carboxyl group ( $-\text{COOH}/$   
197  $\text{COO}^-$ ) was instrumental in catalyzing PHB depolymerization, possibly via a mechanism similar  
198 to that proposed for pyrolysis reactions where cleavage of polyester bonds is initiated by attacking  
199 the  $\alpha$ -hydrogen of the ester group (Reaction 1).<sup>40</sup> The higher reactivity of the deprotonated  
200 carboxylic acids was likely due to the greater bonding potential from absence of hydrogen.<sup>38,40</sup>

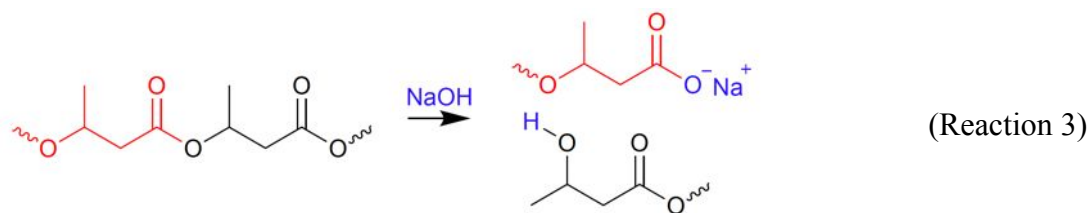


201 Although PHB depolymerization was observed under a variety of conditions, ratios of the  
 202 resulting monomer acid concentration – [3HBA]:[CA] – varied greatly. The observed ratios were  
 203 relatively constant favoring 3HBA for reactions initiated in deionized water (3.0–3.5 for 0.1–1 M  
 204 PHB reacted at 200°C for 2 h). The ratio increased further to 4.7–10.3 when acidic solutions were  
 205 introduced. In contrast, the ratio decreased to 1.6 for reaction in 1 N NaOH, and CA became the  
 206 major product in reactions conducted in neutral-pH solutions amended with the sodium salts of  
 207 formic or butyric acid (the ratio being 0.5 and 0.4, respectively). This was noteworthy as CA was  
 208 reported to be the dominant monomer product observed for pyrolysis of PHB,<sup>38,40</sup> and selectivity  
 209 of monomers has been largely overlooked in earlier reports of PHB depolymerization under  
 210 hydrothermal conditions.

211 The variable monomer selectivity is consistent with multiple mechanisms controlling PHB  
 212 depolymerization. Under acidic conditions, depolymerization may proceed predominantly via the  
 213 reverse of Fischer esterification with 3HBA being the main product (Reaction 2)<sup>46</sup>:



214 Under basic conditions, the reaction likely proceeds predominantly via the saponification pathway  
 215 with salt of 3HBA being the main product (Reaction 3):<sup>46,47</sup>



216 Meanwhile, under both acid and basic conditions, the generated carboxyl groups can further  
217 catalyze the depolymerization reaction via mechanism shown in Reaction 1 (CA as the main  
218 product). As the deprotonated carboxyl terminal groups generated under basic conditions leads to  
219 faster Reaction 1 than the protonated carboxyl terminal groups generated under acidic conditions  
220 (observed in earlier experiments), more CA (from Reaction 1) will be generated under basic  
221 conditions than under acid conditions, leading to a lower [3HBA]:[CA] ratio. It should be noted  
222 that under the investigated conditions, ion product of water could increase to  $10^{-12}$ – $10^{-11}$  mol<sup>2</sup>·L<sup>-2</sup>  
223 (2–3 orders of magnitude higher than at ambient condition),<sup>30</sup> which would significantly increase  
224 the concentrations of H<sup>+</sup> and OH<sup>-</sup> and promote both acid- and base-catalyzed hydrolysis. However,  
225 the acid-catalyzed mechanism has been reported as the dominate one,<sup>30</sup> which may contribute to  
226 the higher selectivity toward 3HBA when water is used as the aqueous medium with no  
227 amendments. This link between amendments, controlling reaction mechanism, and [3HBA]:[CA]  
228 ratio is important as it allows for the selection of one monomer over the other, which can promote  
229 desired PHB-to-propylene conversion by selecting for the monomer acid that is more readily  
230 converted to propylene at lower reaction temperatures (**Section 3.2**).

231

**Table 1** Hydrothermal depolymerization of PHB<sup>a</sup>

T (°C)	[PHB] <sub>0</sub> <sup>b</sup>	Aqueous Solution	Yield (C%) <sup>c</sup>			
			Residual PHB	Oligomers	3HBA	CA
<i>Effect of Reaction Temperature</i>						
175			98.6±0.3%	0.7±0.1%	0%	0%
200			55.3±2.9%	23.3±3.4%	10.5±1.4%	3.5±0.2%
205	0.5	DI water	42.6±0.9%	28.4±0.4%	15.8±0.2%	5.2±0.1%
210			23.4±0.8%	26.9±0.3%	27.4±0.04%	9.2±0.03%
215			0.9±0.2%	24.2±0.9%	38.0±0.8%	18.2±0.4%
220			1.4±0.2%	16.5±0.9%	41.1±0.4%	19.2±0.03%
<i>Effect of Initial PHB Concentration</i>						
	0.1		52.9±1.2%	24.0±2.9%	9.4±2.4%	2.7±0.2%
	0.25		60.3±6.9%	20.5±4.9%	6.4±1.8%	2.1±0.4%
200	0.5	DI water	55.3±2.9%	23.3±3.4%	10.5±1.4%	3.5±0.2%
	0.75		54.5±2.5%	23.1±3.9%	14.2±1.5%	4.5±0.4%
	1		54.4±0.7%	20.6±2.4%	11.2±0.8%	3.6±0.3%
<i>Effect of Aqueous Medium</i>						
		DI water (pH <sub>0</sub> <sup>d</sup> = 6.97)	55.3±2.9%	23.3±3.4%	10.5±1.4%	3.5±0.2%
		0.5 M 3HBA (pH <sub>0</sub> = 2.33)	34.5±0.7%	0%	e	e
		0.5 M CA (pH <sub>0</sub> = 2.47)	12.8±1.6%	0%	e	e
		0.005 M H <sub>2</sub> SO <sub>4</sub> (pH <sub>0</sub> = 2.03)	47.8±7.1%	19.9±2.4%	17.2±1.2%	1.7±0.2%
		0.0005 M H <sub>2</sub> SO <sub>4</sub> (pH <sub>0</sub> = 3.01)	73.3±2.8%	15.5±2.6%	4.6±0.6%	1.0±0.1%
200	0.5	0.5 M Na3HBA <sup>f</sup> (pH <sub>0</sub> = 7.00)	7.1±1.3%	0%	e	e
		0.5 M NaCA <sup>f</sup> (pH <sub>0</sub> = 7.00)	10.6±3.3%	0%	e	e
		0.5 M NaBA <sup>f</sup> (pH <sub>0</sub> = 7.02)	25.2±7.3%	0%	22.0±0.3%	56.9±0.1%
		0.5 M NaFA <sup>f</sup> (pH <sub>0</sub> = 7.09)	0.6±0.6%	0%	28.7±0.7%	60.7±2.6%
		0.5 M H <sub>2</sub> SO <sub>4</sub> (pH <sub>0</sub> = 0)	0%	5.7±4.7%	73.9±2.4%	12.9±0.3%
		1 M NaOH (pH <sub>0</sub> = 14)	1.4±0.4%	9.2±1.7%	53.9±0.3%	33.3±1.7%

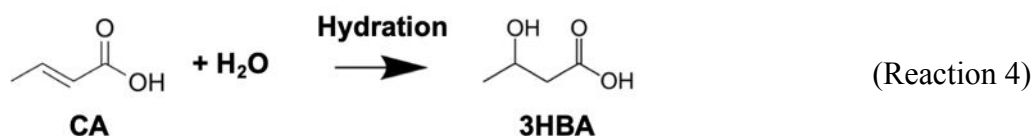
<sup>a</sup> Reaction time was 2 h for all runs; all experiments were conducted in at least duplicate.<sup>b</sup> Initial PHB polymer loading as mol·L<sup>-1</sup> of monomers (solid/liquid).<sup>c</sup> Yields shown in carbon contents expressed as percentages of the initially loaded carbon.<sup>d</sup> pH of aqueous medium prior to reaction.<sup>e</sup> Concentration of 3HBA/CA species not shown due to their pre-existence in the initial aqueous reaction solution and difficulties in determining their origin (i.e., from depolymerization of PHB or amendments).<sup>f</sup> Na3HBA, NaCA, NaBA, and NaFA refer to 3HBA, CA, butyric acid, and formic acid solutions neutralized with NaOH prior to reaction, respectively.

### 232 3.2. (De)hydration and decarboxylation of monomers

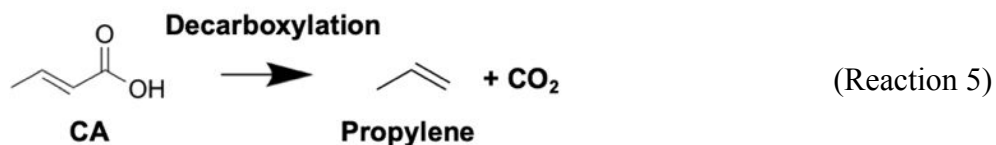
233 While 2-h reactions of PHB at temperatures  $\leq 220^\circ\text{C}$  principally result in depolymerization to  
 234 3HBA and CA, reactions for longer times and/or higher temperatures led to further conversion of  
 235 the monomer acids into propylene and  $\text{CO}_2$ . Thus, further experiments were then undertaken to  
 236 specifically examine reactions of the two monomer acids that occurred under these conditions. In  
 237 general,  $>90\%$  of the initial carbon was recovered as 3HBA, CA, propylene, and  $\text{CO}_2$ , suggesting  
 238 minimal side products and reactions.

#### 239 3.2.1. Crotonic acid (CA)

240 Preliminary experiments initiated with 0.5 M CA revealed no substantial production of  
 241 propylene within 2 h at temperatures  $<250^\circ\text{C}$ , although around 10% of CA underwent hydration  
 242 to 3HBA at the end of experiments, consistent with what was reported in literature (Reaction 4).<sup>48</sup>

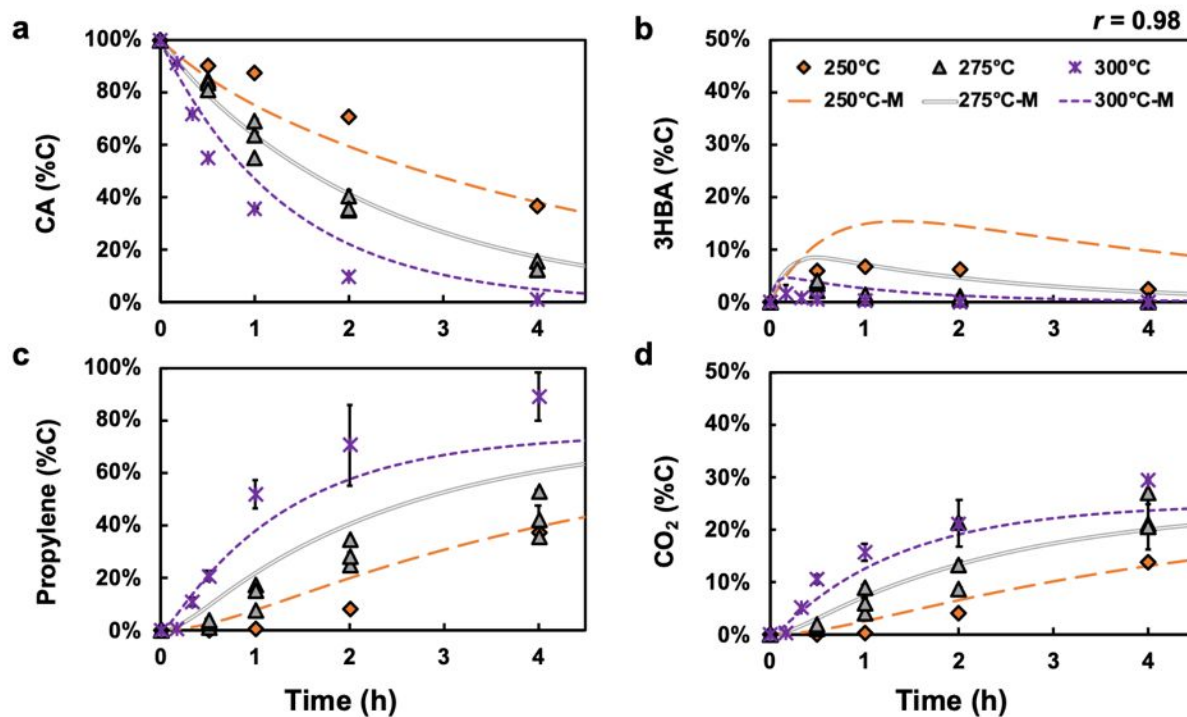


243 Increasing temperatures to  $\geq 250^\circ\text{C}$  led to production of propylene and  $\text{CO}_2$  at approximately  
 244 theoretical ratios (1:1 on molar basis and 3:1 on carbon basis, **Figure 2**), indicating onset of CA  
 245 decarboxylation in addition to hydration (Reaction 5).



246 Reaction rates increased with temperature and near complete conversion of CA to propylene and  
 247  $\text{CO}_2$  was observed within 4 h at  $300^\circ\text{C}$ . 3HBA was observed as a transient intermediate (**Figure**  
 248 **2b**) with peak concentrations occurring earlier and at lower maximum values with increasing  
 249 temperature. This was expected to be the net result of CA hydration and subsequent 3HBA

250 conversion (Section 3.2.2). Separate experiments showed minimal influence of the initial CA  
 251 concentration (0.25–0.75 M at 275°C) on the apparent reaction kinetics and the resulting product  
 252 selectivity, similar to PHB depolymerization.

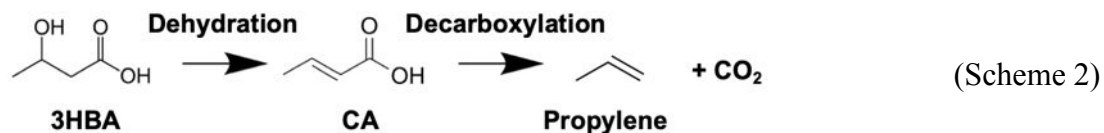


253  
 254 **Figure 2.** Experimental measurements (discrete symbols) and model predictions (lines, Eqs. 2–5)  
 255 for conversion of 0.5 M CA at 250–300°C. Yields are expressed as percentages of the initial loaded  
 256 carbon. The Pearson correlation coefficient<sup>49</sup>  $r$  shown in the upper right evaluates the linear  
 257 correlation between predicted values and experimental measurements for all points in a–d. Error  
 258 bars for duplicate experiments represent min/max measured values and are smaller than symbols  
 259 if not visible.

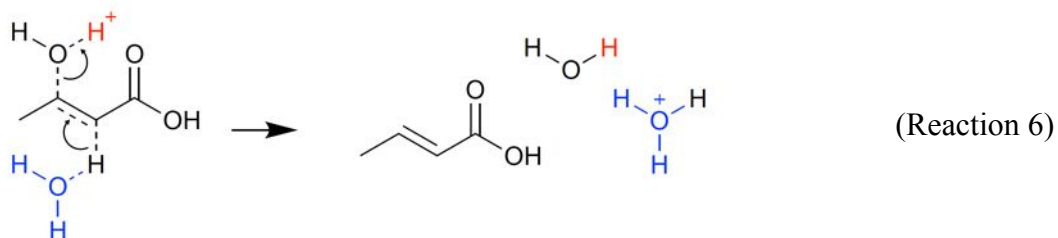
### 260 3.2.2. 3-hydroxybutyric acid (3HBA)

261 Dehydration of 3HBA to CA was observed at temperatures  $\geq 200^\circ\text{C}$ . The conversion of 3HBA  
 262 to CA at low temperatures was expected as it had been reported as the initial step in 3HBA  
 263 conversion during pyrolysis, which was proposed to be followed by decarboxylation of the  
 264 generated CA to propylene and  $\text{CO}_2$  (Scheme 2)<sup>40</sup>:





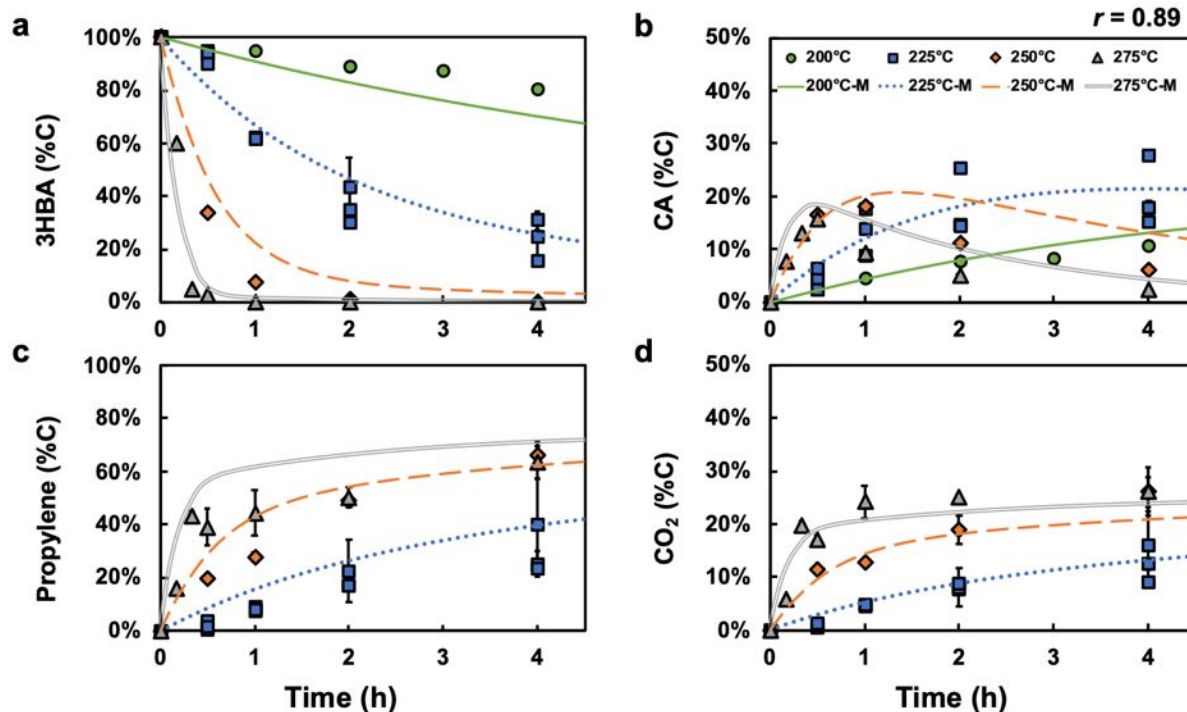
265 Under hydrothermal conditions, 3HBA dehydration could follow the traditional E1 elimination  
 266 mechanism with the trans isomer of CA being the dominant product (Reaction 6):



267 Based on the sequential reactions depicted in Scheme 2, gas production was not expected  
 268 below 250°C – the lowest temperature at which CA was observed to be converted into propylene  
 269 and CO<sub>2</sub> as discussed in the previous section (**Figures 2c** and **2d**). It was thus not expected that >50%  
 270 of 3HBA was converted to propylene and CO<sub>2</sub> (at the theoretical 1:1 molar ratio) when temperature  
 271 was increased to 225°C, with CA (from dehydration reaction) being a minor product. Therefore,  
 272 decomposition of 3HBA to gas products occurred at lower temperatures and faster rates than CA  
 273 (i.e., rate of propylene and CO<sub>2</sub> formation from 3HBA at 225°C > rate from CA at 250°C). The  
 274 inconsistency between this finding and the sequential dehydration and decarboxylation pathway  
 275 (Scheme 2) suggests an alternative lower-temperature pathway for 3HBA conversion to propylene  
 276 (**Section 3.3**).

277 Experiments conducted at higher temperatures revealed a sharp increase in rates of 3HBA  
 278 conversion. While only 20% of 3HBA was converted after 4 h of reaction at 200°C, complete  
 279 conversion was achieved within 0.5 h at 275°C (**Figure 3a**). Formation of the dehydration product  
 280 CA also depended heavily on the temperature. For reactions at 200 and 225°C, concentration of

281 CA increased throughout the time studied; whereas for reactions conducted at 250 and 275°C, CA  
 282 concentration first increased to around 20% before decreasing (**Figure 3b**). This can be explained  
 283 by the net effects of CA formation by dehydration of 3HBA and decomposition of the generated  
 284 CA to gas products. At 200 and 225°C, 3HBA had not been fully converted within the time range  
 285 monitored (4 h); but at 250 and 275°C, all 3HBA had been converted within 1 h, and no additional  
 286 CA was generated afterward. Meanwhile, further conversion of CA to propylene and CO<sub>2</sub> only  
 287 became appreciable at  $\geq 250^\circ\text{C}$ . In fact, concentration of CA started to decrease at 1 h for 250°C  
 288 and 0.5 h for 275°C, corresponding with times at which 3HBA was nearly depleted. Likewise,  
 289 rates of propylene and CO<sub>2</sub> production slowed after 3HBA was depleted, indicating that the faster  
 290 3HBA-to-gas pathway had ceased, but slower conversion of the residual CA continued (**Figures**  
 291 **3c** and **3d**). Finally, further tests showed that, like kinetics for PHB and CA conversion, the kinetics  
 292 of 3HBA conversion were independent of its initial concentration (0.25–0.75 M at 225°C).

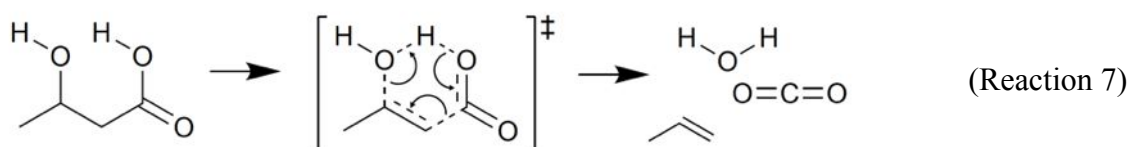


293

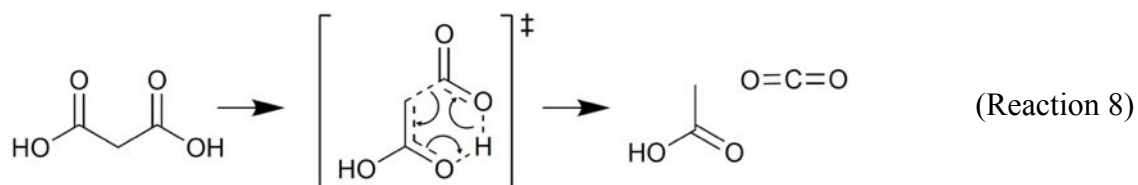
294 **Figure 3.** Experimental measurements (discrete symbols) and model predictions (lines, Eqs. 2–5)  
 295 for conversion of 0.5 M 3HBA at 200–275°C. Yields are expressed as percentages of the initial  
 296 loaded carbon. The Pearson correlation coefficient<sup>49</sup>  $r$  shown in the upper right evaluates the linear  
 297 correlation between predicted values and experimental measurements for all points in a–d. Error  
 298 bars for duplicate experiments represent min/max measured values and are smaller than symbols  
 299 if not visible.

### 300 3.3. Reaction mechanism

301 Synthesizing these observations together with the fact that no aqueous species other than  
 302 3HBA and CA were detected in significant yields (>4%), a new mechanism was proposed for  
 303 conversion of 3HBA to propylene and CO<sub>2</sub> (Reaction 7):

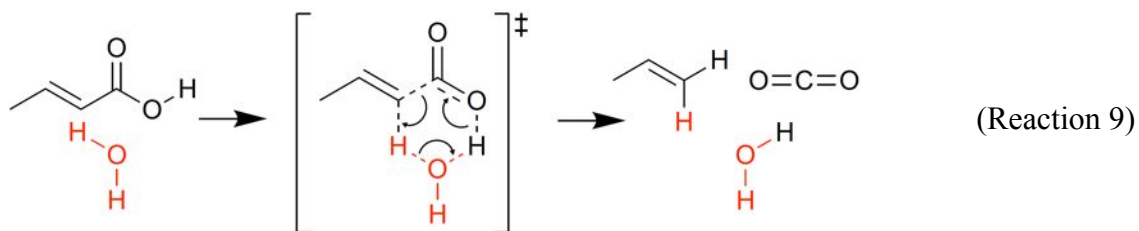


304 where dehydration and decarboxylation of 3HBA occurs in a concerted fashion (concerted DHYD-  
 305 DCXY), thereby bypassing production of CA as an intermediate (Scheme 2, proposed mechanism  
 306 for pyrolysis<sup>40</sup>). It is proposed that the reaction proceeds through an intramolecular 6-member ring  
 307 transition state formed by hydrogen bonding between oxygen in the hydroxy group and hydrogen  
 308 in the protonated carboxyl group. A similar mechanism has been proposed for decarboxylation of  
 309  $\beta$ -keto acids under hydrothermal conditions, where the cyclic transition state weakens the C-  
 310 COOH bond (e.g., decarboxylation of malonic acid shown in Reaction 8).<sup>50–52</sup>



311 It should be noted that 3HBA must be protonated for the concerted reaction to proceed, which is  
 312 supported by minimal (<2%) amounts of propylene and CO<sub>2</sub> formation when sodium salt of 3HBA  
 313 was used as the initial reactant (225 and 275°C, 0.5 M, 2 h).

314 As conversion of CA and generation of gas products followed (pseudo-) first-order rate law  
 315 (**Figure 2**), conversion of CA can either proceed through direct decarboxylation catalyzed by water  
 316 (Reaction 9):



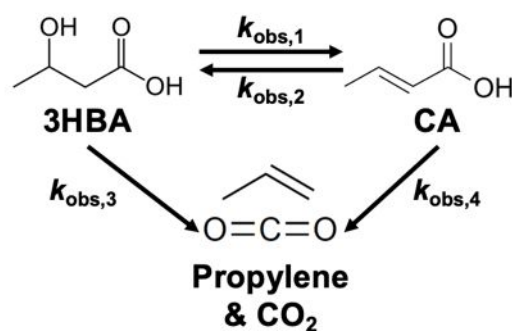
317 or through a two-step process where hydration to 3HBA is followed by concerted DHYD-DCXY  
 318 of the generated 3HBA (Scheme 3):



319 For the direct decarboxylation route, hydrogen bonding with water forms a 6-member ring  
 320 transition state that weakens the C-C bond between the carboxyl group and the  $\alpha$ -carbon atom,  
 321 leading to heterolytic cleavage and formation of the terminal alkene and CO<sub>2</sub>. In fact, any  
 322 molecules with a hydroxy group can catalyze the reaction via this proposed mechanism (e.g.,  
 323 3HBA from hydration of CA), but water is expected to be the main contributor due to its ubiquity  
 324 at the studied conditions (molarity of water >100 times of CA for 0.5 M CA solution). Previous  
 325 studies have reported the effects of water on decarboxylation reactions at similar conditions,<sup>52-54</sup>  
 326 with computational studies suggesting water-involved cyclic transition state can lower the  
 327 activation energy.<sup>53,54</sup> Similar to the concerted DHYD-DCXY pathway of 3HBA, CA must be in  
 328 its protonated form for the reaction to proceed via the proposed pathway in Reaction 9, which is  
 329 supported by the fact that <4% of propylene and CO<sub>2</sub> were observed during experiment initiated

330 with the sodium salt of CA at 275°C (0.5 M, 2h). The relative importance of the two potential  
 331 pathways for CA conversion to gas products was investigated with kinetics modeling (**Section 3.4**).

332 To sum up, it is proposed that conversion of PHB monomers 3HBA and CA mainly proceed  
 333 through four reactions: (1) dehydration of 3HBA to CA, (2) hydration of CA to 3HBA, (3)  
 334 concerted DHYD-DCXY of 3HBA to propylene and CO<sub>2</sub>, and (4) direct decarboxylation of CA  
 335 to propylene and CO<sub>2</sub> (Scheme 4).



(Scheme 4)

### 336 3.4. Kinetics model

337 A kinetics model was developed to provide quantitative support for the proposed reaction  
 338 network depicted in Scheme 4. The kinetics of individual reactions were assumed to follow  
 339 (pseudo-) first-order rate law, and concentration of each species (denoted as [C<sub>Species</sub>]) expressed  
 340 on carbon basis can be described as:

$$341 \quad \frac{d[C_{3HBA}]}{dt} = -(k_{obs,1} + k_{obs,3})[C_{3HBA}] + k_{obs,2}[C_{CA}] \quad (\text{Eq. 2})$$

$$342 \quad \frac{d[C_{CA}]}{dt} = -(k_{obs,2} + k_{obs,4})[C_{CA}] + k_{obs,1}[C_{3HBA}] \quad (\text{Eq. 3})$$

$$343 \quad \frac{d[C_{Propylene}]}{dt} = \frac{3}{4}(k_{obs,3}[C_{3HBA}] + k_{obs,4}[C_{CA}]) \quad (\text{Eq. 4})$$

$$344 \quad \frac{d[C_{CO_2}]}{dt} = \frac{1}{4}(k_{obs,3}[C_{3HBA}] + k_{obs,4}[C_{CA}]) \quad (\text{Eq. 5})$$

345 Next, least-squares objective function was used to fit the experimental data (concentration of  
 346 3HBA, CA, propylene, and CO<sub>2</sub> from conversion of 0.5 M 3HBA at 200–275°C or 0.5 M CA at  
 347 250–300°C) and determine values of the four apparent rate constants at each reaction temperature.  
 348 The resulting “Fitted” rate constants are summarized in **Table 2**. Initially, all rate constants were  
 349 freely adjusted during fits with the exception of  $k_{\text{obs},3}$  at 200°C and  $k_{\text{obs},4}$  at 200 and 225°C, which  
 350 were fixed at 0 as minimal gas products were observed during experiments for 3HBA ( $k_{\text{obs},3}$ ) and  
 351 CA ( $k_{\text{obs},4}$ ) reactions. However, the fit-derived values of  $k_{\text{obs},4}$  were found to negligible ( $\leq 0.08 \text{ h}^{-1}$ )  
 352 compared to other rate constants, indicating that direct CA decarboxylation (Reaction 9) was not  
 353 important and that the alternative pathway depicted in Scheme 3 (CA hydration to 3HBA followed  
 354 by concerted DHYD-DCXY) predominated. As a result, model fitting was re-performed after  
 355 excluding  $k_{\text{obs},4}$  for all reaction temperatures (i.e., value fixed at 0). The resulting values of  $k_{\text{obs},1}$ ,  
 356  $k_{\text{obs},2}$ , and  $k_{\text{obs},3}$  were similar to values determined when  $k_{\text{obs},4}$  was included during fitting  
 357 (differences  $\leq 0.11 \text{ h}^{-1}$ ), supporting elimination of the direct CA decarboxylation pathway from the  
 358 reaction network.

359 **Table 2** Rate constants and fitted kinetics parameters<sup>a</sup>

$k_{\text{obs}}$ [ $\text{h}^{-1}$ ] <sup>b</sup>	T (°C)					$E_a$ ( $\text{kJ}\cdot\text{mol}^{-1}$ )	lnA	$r^2$	
	200	225	250	275	300				
$k_{\text{obs},1}$	Fitted	0.05±0.01	0.14±0.04	0.49±0.05	1.16±0.19	NA <sup>c</sup>	92.2±3.4	20.4±0.8	1.00
	Calculated	0.05	0.16	0.45	1.19	2.88			
$k_{\text{obs},2}$	Fitted	0.12±0.15	0.18±0.17	0.26±0.03	0.56±0.01	1.03±0.02	48.4±5.5	10.0±1.3	0.96
	Calculated	0.10	0.19	0.34	0.56	0.89			
$k_{\text{obs},3}$	Fitted	NA <sup>d</sup>	0.25±0.01	1.23±0.03	3.18±0.43	15.47±0.81	126.8±9.2	29.2±2.1	0.99
	Calculated	0.05	0.25	1.08	4.07	13.69			

<sup>a</sup> Data for reactions of 0.5 M 3HBA or CA at different temperatures (**Figures 2 and 3**) were fitted with Eqs 2–5.

<sup>b</sup> “Fitted” parameters were obtained by least-squares fitting with  $k_{\text{obs},3}$  at 200°C and all  $k_{\text{obs},4}$  values fixed at 0 (negligible at the studied temperatures); “Calculated” parameters were determined by linear regression of the Arrhenius parameters (Eq. 1) to the “Fitted” rate constant values.

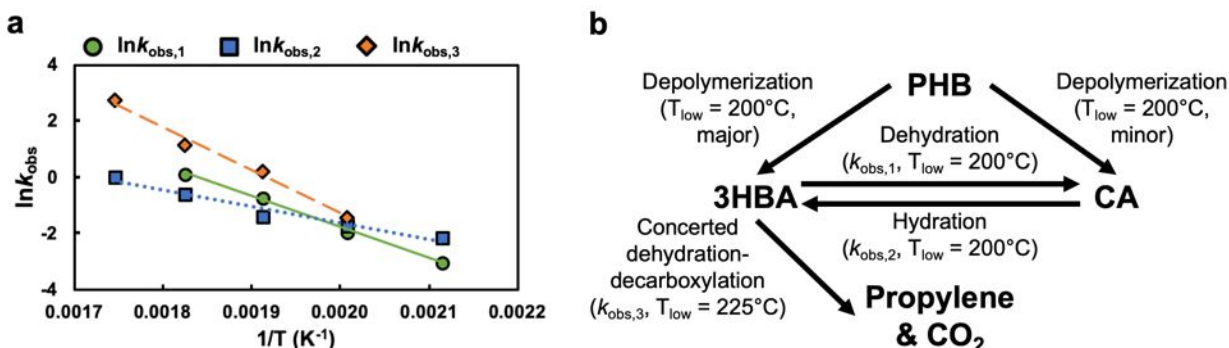
<sup>c</sup> Value fitted to be 0 by algorithm.

<sup>d</sup> Value fixed at 0 during fitting because the reaction in question was not observed at this temperature.

360 Based on the results in **Table 2**, both dehydration and hydration reaction were slow at 200°C,  
361 but the rate constant for CA hydration reaction ( $k_{\text{obs},2}$ ) was larger than that for 3HBA dehydration  
362 ( $k_{\text{obs},1}$ ), consistent with experimental results where more 3HBA was generated from CA  
363 ( $16.4\pm 0.6\%$ ) than CA from 3HBA ( $7.4\pm 0.3\%$ ). When temperature increased to 225°C and above,  
364 however, the concerted DHYD-DCXY pathway predominated the consumption of 3HBA, with  
365  $k_{\text{obs},3} \gg k_{\text{obs},1}$  and  $k_{\text{obs},2}$ . At 300°C, reaction of 3HBA yielded negligible amounts of CA in  
366 comparison with propylene and CO<sub>2</sub>, so  $k_{\text{obs},1}$  was excluded from the fit of data collected at this  
367 temperature.

368 The fitted (pseudo-) first-order rate constants for the 3HBA dehydration, CA hydration, and  
369 concerted DHYD-DCXY of 3HBA reactions ( $k_{\text{obs},1}$ – $k_{\text{obs},3}$ ) measured at 200–300°C (**Table 2**,  
370 “Fitted” values) were used to derive apparent activation energies ( $E_a$ , kJ·mol<sup>-1</sup>) and pre-exponential  
371 factors (A) from least-squares fitting of the Arrhenius equation (Eq. 1; **Figure 4a**, **Table 2**). The  
372 Arrhenius parameters were then used to back-calculate rate constants each temperature, including  
373 conditions where no rate constant could be directly observed (e.g.,  $k_{\text{obs},1}$  at 300°C) (**Table 2**,  
374 “Calculated” values). The Arrhenius “Calculated” values generally agree closely with the “Fitted”  
375 values. Further validation of the kinetics network model and the Arrhenius activation parameters  
376 is provided by close agreement between measurements and predictions of the concentration  
377 profiles for CA, 3HBA, propylene and CO<sub>2</sub> measured at different temperatures (Pearson  
378 correlation coefficient<sup>49</sup> is 0.98 for CA and 0.89 for 3HBA, see model predictions in **Figures 2**  
379 and **3**). For reactions initiated with 3HBA (**Figure 3**), model predictions agree very closely with  
380 measurements for 3HBA at 225–275°C, CA at 200 and 225°C, propylene at 225°C, and CO<sub>2</sub> at all  
381 temperatures were the most accurate with almost all points falling on or near the predicted lines.  
382 Some deviations were observed for 3HBA at 200°C (underestimation), and CA (overestimation

383 for >1 h) and propylene (overestimation 0.5–2 h) at 250–275°C, but the deviations were not  
 384 significant. Predictions for CA were even more robust with the only significant deviation being  
 385 overprediction of 3HBA at 250°C, which was probably due to the relative low concentrations of  
 386 3HBA forming at these conditions.



387  
 388 **Figure 4.** (a) Fits of the Arrhenius equation (Eq. 1) for dehydration of 3HBA ( $k_{\text{obs},1}$ ), hydration of  
 389 CA ( $k_{\text{obs},2}$ ), and concerted DHYD-DCXY of 3BHA ( $k_{\text{obs},3}$ ). The resulting activation parameters  
 390 and fit qualities are provided in **Table 2**. (b) Proposed reaction network for PHB-to-propylene  
 391 conversion.  $T_{\text{low}}$  indicates the lowest temperature at which each reaction was observed in this study.

392 **Figure 4b** summarizes the principal reaction pathways and lowest observed temperature ( $T_{\text{low}}$ )  
 393 for each reaction. According to this reaction network, hydrothermal depolymerization of PHB  
 394 occurs at temperatures  $\geq 200^\circ\text{C}$ , with a predominance of 3HBA over CA (DI water as the aqueous  
 395 medium without amendments). The monomer acids are interconvertible by (de)hydration reactions.  
 396 At  $\geq 225^\circ\text{C}$ , 3HBA is converted to propylene and  $\text{CO}_2$  via the concerted DHYD-DCXY pathway,  
 397 and experiments and modeling demonstrate that CA conversion to the same products occurs by  
 398 sequential hydration to 3HBA followed by the concerted DHYD-DCXY pathway. These reactions  
 399 occur at temperatures lower than those typically used for hydrothermal liquefaction of biomass for  
 400 biocrude oil and co-products,<sup>55</sup> suggesting a strategy for selective production of propylene when  
 401 hydrothermally processing PHB-containing biomass.



### 402 3.5. Conversion of PHB-containing biomass

403 As a demonstration and validation of the proposed reaction network, PHB-containing biomass  
404 was subjected to hydrothermal processing at conditions similar to those used for processing  
405 commercially sourced PHB and its monomer acids. The biomass was cultivated in a pilot-scale  
406 (500 L) reactor using natural gas as the methane source and was a mixed culture dominated by  
407 Type II methanotrophs. The biomass had a PHB content of  $41.2 \pm 0.7\%$  with  $51.9 \pm 0.2\%$  C,  $7.2 \pm 0.02\%$   
408 H,  $5.0 \pm 0.04\%$  N, and  $36.0 \pm 0.2\%$  O, and an ash content of  $7.7 \pm 0.2\%$  (all on dry weight basis),  
409 which were comparable to those previously reported for methanotrophs.<sup>10,56</sup> Conversion was first  
410 conducted at  $275^\circ\text{C}$  for 4 h since the kinetics model predicted that this condition would be  
411 sufficient for complete depolymerization of PHB and conversion of both 3HBA and CA to  
412 propylene and  $\text{CO}_2$ . As expected, all PHB in the biomass was converted to propylene and  $\text{CO}_2$  at  
413 close-to-theoretical ratio (**Table 3**, Run 1). This was notable as previous reports of PHB-to-  
414 propylene were conducted at higher temperatures ( $300\text{--}375^\circ\text{C}$  for hydrothermal conversion,<sup>28,29,57</sup>  
415  $350\text{--}450^\circ\text{C}$  for pyrolysis<sup>40,58</sup>). Interestingly, when a higher reaction temperature was used, less  
416 propylene was observed despite complete conversion of PHB and its monomers (**Table 3**, Run 2),  
417 and the sum of 3HBA, CA, propylene, and  $\text{CO}_2$  were only  $74.3 \pm 7.0\%$  compared to  $93.8 \pm 7.5\%$  at  
418  $275^\circ\text{C}$ . Since the yield of  $\text{CO}_2$  remained unchanged, this was attributed to reactions between  
419 propylene and non-PHB cellular materials (NPCMs), or ketonization reactions between 3HBA/CA  
420 and NPCM derivatives that would generate  $\text{CO}_2$  but not propylene.<sup>32,59,60</sup> Hydrothermal conversion  
421 of NPCMs may involve depolymerization of large biomacromolecules (e.g., proteins to amino  
422 acids, triacylglycerides to fatty acids, carbohydrates to sugars), decomposition of the generated  
423 monomers (e.g., decarboxylation, deamination, dehydration of amino acids), and further reactions  
424 between the monomers and derivative products (e.g., amides from amino acids and fatty acid esters,

425 melanoidins from Maillard reactions of amino acids and sugars).<sup>59</sup> Reactions between acids and  
 426 alkenes (highly reactive due to the presence of carboxylic group and/or double bond) produced  
 427 from hydrothermal conversion of medium chain-length PHA and NPCMs have been observed, but  
 428 mechanisms of these reactions have not been examined.<sup>32</sup> It follows that lower reaction  
 429 temperatures not only reduce heating energy requirements, but also maximize propylene yields by  
 430 reducing losses to biocrude/aqueous products due to reactions with NPCM derivatives.

431 **Table 3** Hydrothermal conversion of PHB-containing biomass<sup>a</sup>

Run #	T (°C)	t (h)	Aqueous Medium	Yield (C%) <sup>b</sup>			
				3HBA	CA	Propylene	CO <sub>2</sub>
1	275	4	DI water	0%	0%	69.5±4.2%	24.3±6.2%
2	350	1	DI water	0%	0%	53.5±6.2%	20.8±3.3%
3	250	2	DI water	5.0±0.3%	36.6±2.0%	38.2±2.6%	13.2±0.1%
4	250	4	DI water	2.7±0.4%	20.1±1.4%	54.0±2.2%	19.4±2.2%
5	250	6	DI water	2.5±0.2%	14.3±1.6%	61.4±4.9%	23.6±1.2%
6	250	4	0.005 M H <sub>2</sub> SO <sub>4</sub>	2.6±0.1%	20.3±0.8%	42.5±12.8%	15.5±3.8%
7	250	4	0.05 M H <sub>2</sub> SO <sub>4</sub>	3.5±0.1%	30.5±0.4%	37.8±2.2%	13.3±1.5%
8	250	4	DI water	2.4±0.2%	28.9±0.3%	35.6±3.3%	10.1±1.1%

<sup>a</sup> All experiments were started with 86.1 mg of solids and 2 mL of aqueous solution, which was an equivalent of 0.5 M (as PHB monomers) assuming the solid was 100% PHB; PHB-containing biomass was used for Runs 1–7 and commercially sourced PHB was used for Run 8. All experiments were performed in duplicate.

<sup>b</sup> Yields shown in carbon contents expressed as percentages of initially loaded PHB.

432 Experiments were then conducted at 250°C to gauge the potential for further lowering reaction  
 433 temperatures. Within 2 h, half of the intracellular PHB had decomposed to propylene and CO<sub>2</sub>  
 434 with near-complete conversion of 3HBA, but around 40% of CA remained (**Table 3**, Run 3). When  
 435 the reaction was extended to 4 and 6 h, the CA gradually decomposed and around 80% of the  
 436 initial PHB was converted to propylene and CO<sub>2</sub> (**Table 3**, Runs 4 and 5). To further accelerate  
 437 the conversion via the faster concerted DHYD-DCXY of 3HBA, additional experiments were also  
 438 performed with acid solution as the aqueous medium instead of water, as earlier data revealed  
 439 higher selectivity to 3HBA during depolymerization of PHB under acidic conditions. However,  
 440 use of acid solutions decreased rates of PHB conversion and yields of propylene and CO<sub>2</sub> (**Table**

441 **3**, Runs 6 and 7), and the sum of 3HBA, CA, propylene, and CO<sub>2</sub> decreased to 80–85%, indicating  
442 potential loss to interactions with NPCM derivatives that can be catalyzed by the added acids.<sup>61</sup>  
443 Interestingly, experiments also showed that intracellular PHB was depolymerized more rapidly  
444 than commercially sourced PHB granules subjected to the same hydrothermal conditions (**Table**  
445 **3**, Runs 4 and 8), and the sum of 3HBA, CA, propylene, and CO<sub>2</sub> for pure PHB was only  
446 77.0±3.5%, suggesting incomplete conversion of oligomers and slower kinetics. The faster  
447 conversion of intracellular PHB might be a result of its amorphous elastomeric state,<sup>62</sup> which can  
448 be lost upon extraction from the cells,<sup>63</sup> or due to the interactions between the intracellular PHB,  
449 its monomers, and NPCMs that either favors production of 3HBA (from depolymerization of PHB  
450 or hydration of CA) or inhibits the dehydration of 3HBA to CA. These results highlight the needs  
451 to examine the role of NPCMs and their derivatives in hydrothermal conversion of PHB at varying  
452 conditions and corresponding mechanisms, which should be addressed in future research. Still,  
453 findings from this work demonstrate effective conversion of intracellular PHB to near-theoretical  
454 yields of propylene at temperatures significantly lower than past reports. This provides a promising  
455 pathway forward for enhanced valorization of wastewater organic carbon sources.

### 456 **3.6. Broader impacts**

457 With waste valorization through biorefineries attracting increased attention,<sup>64–66</sup> there is  
458 growing interest in identifying promising strategies for resource recovery from waste organic  
459 streams.<sup>2,3,67</sup> Herein, hydrothermal conversion of wastewater-derived PHB is proposed for  
460 generation of propylene, which in turn can be used for production of liquid fuels (e.g., C<sub>6</sub>–C<sub>12</sub>  
461 hydrocarbons via oligomerization<sup>68</sup>) or other higher-value chemicals (e.g., cumene,<sup>69</sup>  
462 propanediol<sup>70</sup>). As the market for propylene is projected to grow in the future and North America  
463 is predicted to be one of the largest markets,<sup>71</sup> wastewater is an appealing source to meet these

464 demands in a more sustainable and cost-effective manner. With developments in biocatalysts,  
465 polyhydroxyalkanoates (PHAs) with higher molecular weight monomers (e.g.,  
466 polyhydroxyvalerate<sup>72</sup>) can also be synthesized. Under hydrothermal conditions, these PHAs are  
467 expected to go through similar reactions: the depolymerization and (de)hydration pathways are  
468 viable for all PHAs and their monomers, and the concerted DHYD-DCXY pathway is viable for  
469 any PHA monomers containing a  $\beta$ -hydroxy group, which are commonly produced by  
470 microorganisms.<sup>73</sup> Therefore, longer renewable alkenes with broader applications could be  
471 produced in a similar manner.<sup>32</sup> In addition, the concerted DHYD-DCXY pathway is particularly  
472 interesting as it provides the possibility to bypass direct decarboxylation of unsaturated carboxylic  
473 acids, which proceeds at much lower rates compared to saturated fatty acids.<sup>65,74</sup> Moreover,  
474 mechanistic insights concluded in this study can be applied to determine optimal reaction  
475 conditions for converting PHB-containing biomass. The lower reaction temperatures are not only  
476 beneficial in reducing capital and operating costs, but also result in higher propylene yields by  
477 avoiding the incorporation of propylene into biocrudes or aqueous products generated from  
478 hydrothermal liquefaction of NPCMs.

#### 479 **4. Conclusions**

480 In this work, hydrothermal conversion of PHB and its monomers 3HBA and CA were studied  
481 for production of propylene from wastewater-derived biomass. It was concluded that under  
482 hydrothermal conditions, PHB would first depolymerize into a mixture of 3HBA and CA, which  
483 would dehydrate and decarboxylate into propylene and CO<sub>2</sub>. Selectivity of PHB depolymerization  
484 was found to be greatly affected by aqueous media: while 3HBA was the major product in water  
485 without amendments or with addition of mineral acids, addition of mineral base decreased the  
486 selectivity to 3HBA, and CA would become the major product with carboxyl amendments. This

487 variation in product selectivity was attributed to the dominate depolymerization mechanism that  
488 varied with aqueous amendments but not with initial PHB loading nor reaction temperature.  
489 Further investigation of 3HBA and CA decomposition revealed that 3HBA could be converted to  
490 propylene at lower temperatures and faster rates than CA, and a new concerted DHYD-DCXY  
491 pathway was proposed for 3HBA. A kinetics network model was developed for conversion of PHB  
492 and Arrhenius kinetics parameters were derived for decomposition of 3HBA and CA, which  
493 revealed that conversion of CA to propylene proceeded mainly through hydration to 3HBA  
494 followed by the concerted DHYD-DCXY pathway. Conversion of PHB-containing biomass was  
495 demonstrated at conditions that were milder than previously reported, and near-theoretical  
496 production of propylene was observed, validating conclusions from the kinetics study and the  
497 developed network model.

#### 498 **Conflicts of interest**

499 There are no conflicts to declare.

#### 500 **Acknowledgements**

501 Financial support for work carried out at CSM was provided by National Science Foundation  
502 (NSF) through the NSF Engineering Research Center for Reinventing the Nation's Urban Water  
503 Infrastructure (ReNUWIt; EEC-1028968) and NSF award CBET-1804513. Derek Vardon  
504 (National Renewable Energy Laboratory) is acknowledged for valuable discussions. Allison Pieja  
505 and Yu Kuwabara at Mango Materials are acknowledged for providing PHB-containing biomass.

506 **References**

- 507 1 U.S. EPA, *Energy Efficiency in Water and Wastewater Facilities*, 2013.
- 508 2 W.-W. Li, H.-Q. Yu and B. E. Rittmann, *Nature News*, 2015, **528**, 29.
- 509 3 M. T. Agler, B. A. Wrenn, S. H. Zinder and L. T. Angenent, *Trends Biotechnol.*, 2011, **29**, 70–  
510 78.
- 511 4 R. Kleerebezem, B. Joosse, R. Rozendal and M. C. M. V. Loosdrecht, *Rev Environ Sci*  
512 *Biotechnol*, 2015, **14**, 787–801.
- 513 5 K. Solon, E. I. P. Volcke, M. Spérandio and M. C. M. van Loosdrecht, *Environ. Sci.: Water*  
514 *Res. Technol.*, 2019, **5**, 631–642.
- 515 6 S. Bengtsson, A. Karlsson, T. Alexandersson, L. Quadri, M. Hjort, P. Johansson, F. Morgan-  
516 Sagastume, S. Anterrieu, M. Arcos-Hernandez, L. Karabegovic, P. Magnusson and A. Werker,  
517 *New Biotechnology*, 2017, **35**, 42–53.
- 518 7 F. Morgan-Sagastume, M. Hjort, D. Cirne, F. Gérardin, S. Lacroix, G. Gaval, L. Karabegovic,  
519 T. Alexandersson, P. Johansson, A. Karlsson, S. Bengtsson, M. V. Arcos-Hernández, P.  
520 Magnusson and A. Werker, *Bioresource Technology*, 2015, **181**, 78–89.
- 521 8 E. Korkakaki, M. Mulders, A. Veeken, R. Rozendal, M. C. M. van Loosdrecht and R.  
522 Kleerebezem, *Water Research*, 2016, **96**, 74–83.
- 523 9 H. Salehizadeh and M. C. M. Van Loosdrecht, *Biotechnology Advances*, 2004, **22**, 261–279.
- 524 10 A. J. Pieja, E. R. Sundstrom and C. S. Criddle, *Appl. Environ. Microbiol.*, 2011, **77**, 6012–  
525 6019.
- 526 11 K. Khosravi-Darani, Z.-B. Mokhtari, T. Amai and K. Tanaka, *Appl Microbiol Biotechnol*, 2013,  
527 **97**, 1407–1424.
- 528 12 N. Basset, E. Katsou, N. Frison, S. Malamis, J. Dosta and F. Fatone, *Bioresource Technology*,  
529 2016, **200**, 820–829.
- 530 13 N. Frison, E. Katsou, S. Malamis, A. Oehmen and F. Fatone, *Environ. Sci. Technol.*, 2015, **49**,  
531 10877–10885.
- 532 14 P. J. Strong, S. Xie and W. P. Clarke, *Environ. Sci. Technol.*, 2015, **49**, 4001–4018.
- 533 15 P. J. Strong, M. Kalyuzhnaya, J. Silverman and W. P. Clarke, *Bioresource Technology*, 2016,  
534 **215**, 314–323.
- 535 16 A. J. Pieja, M. C. Morse and A. J. Cal, *Current Opinion in Chemical Biology*, 2017, **41**, 123–  
536 131.
- 537 17 S. Bengtsson, A. Werker, M. Christensson and T. Welander, *Bioresource Technology*, 2008,  
538 **99**, 509–516.
- 539 18 J. Tamis, K. Lužkov, Y. Jiang, M. C. M. van Loosdrecht and R. Kleerebezem, *Journal of*  
540 *Biotechnology*, 2014, **192**, Part A, 161–169.
- 541 19 E. Akaraonye, T. Keshavarz and I. Roy, *Journal of Chemical Technology & Biotechnology*,  
542 2010, **85**, 732–743.
- 543 20 S. Chanprateep, *Journal of Bioscience and Bioengineering*, 2010, **110**, 621–632.
- 544 21 K. Dietrich, M.-J. Dumont, L. F. Del Rio and V. Orsat, *Sustainable Production and*  
545 *Consumption*, 2017, **9**, 58–70.
- 546 22 N. Jacquél, C.-W. Lo, Y.-H. Wei, H.-S. Wu and S. S. Wang, *Biochemical Engineering Journal*,  
547 2008, **39**, 15–27.
- 548 23 A. Aramvash, F. M. Zavareh and N. G. Banadkuki, *Engineering in Life Sciences*, 2018, **18**,  
549 20–28.

- 550 24 C. Pérez-Rivero, J. P. López-Gómez and I. Roy, *Biochemical Engineering Journal*, 2019, **150**,  
551 107283.
- 552 25 J. Mozejko-Ciesielska and R. Kiewisz, *Microbiological Research*, 2016, **192**, 271–282.
- 553 26 J. Yu and L. X. L. Chen, *Biotechnol. Prog.*, 2006, **22**, 547–553.
- 554 27 P. J. Strong, B. Laycock, S. N. S. Mahamud, P. D. Jensen, P. A. Lant, G. Tyson and S. Pratt,  
555 *Microorganisms*, 2016, **4**, 11.
- 556 28 J. Wagner, R. Bransgrove, T. A. Beacham, M. J. Allen, K. Meixner, B. Drogg, V. P. Ting and  
557 C. J. Chuck, *Bioresource Technology*, 2016, **207**, 166–174.
- 558 29 C. Torri, T. D. O. Weme, C. Samori, A. Kiwan and D. W. F. Brilman, *Environ. Sci. Technol.*,  
559 2017, **51**, 12683–12691.
- 560 30 N. Akiya and P. E. Savage, *Chem. Rev.*, 2002, **102**, 2725–2750.
- 561 31 P. E. Savage, *The Journal of Supercritical Fluids*, 2009, **47**, 407–414.
- 562 32 T. Dong, W. Xiong, J. Yu and P. T. Pienkos, *RSC Adv.*, 2018, **8**, 34380–34387.
- 563 33 C. M. Beal, L. N. Gerber, D. L. Sills, M. E. Huntley, S. C. Machesky, M. J. Walsh, J. W.  
564 Tester, I. Archibald, J. Granados and C. H. Greene, *Algal Research*, 2015, **10**, 266–279.
- 565 34 L. N. Gerber, J. W. Tester, C. M. Beal, M. E. Huntley and D. L. Sills, *Environ. Sci. Technol.*,  
566 2016, **50**, 3333–3341.
- 567 35 S. Leow, B. D. Shoener, Y. Li, J. L. DeBellis, J. Markham, R. Davis, L. M. L. Laurens, P. T.  
568 Pienkos, S. M. Cook, T. J. Strathmann and J. S. Guest, *Environ. Sci. Technol.*, 2018, **52**,  
569 13591–13599.
- 570 36 Y. Li, W. A. Tarpeh, K. L. Nelson and T. J. Strathmann, *Environ. Sci. Technol.*, 2018, **52**,  
571 12717–12727.
- 572 37 S. Nguyen, G. Yu and R. H. Marchessault, *Biomacromolecules*, 2002, **3**, 219–224.
- 573 38 H. Ariffin, H. Nishida, Y. Shirai and M. A. Hassan, *Polymer Degradation and Stability*, 2008,  
574 **93**, 1433–1439.
- 575 39 H. Nishida, H. Ariffin, Y. Shirai and M. Hassan, , DOI:10.5772/10270.
- 576 40 J. M. Clark, H. M. Pilath, A. Mittal, W. E. Michener, D. J. Robichaud and D. K. Johnson, *J.*  
577 *Phys. Chem. A*, 2016, **120**, 332–345.
- 578 41 T. Saeki, T. Tsukegi, H. Tsuji, H. Daimon and K. Fujie, *Polymer*, 2005, **46**, 2157–2162.
- 579 42 W. M. Haynes, *CRC Handbook of Chemistry and Physics, 97th Edition*, CRC Press, 97th edn.,  
580 2016.
- 581 43 A. G. Carr, R. Mammucari and N. R. Foster, *Chemical Engineering Journal*, 2011, **172**, 1–17.
- 582 44 J. L. Faeth, P. J. Valdez and P. E. Savage, *Energy Fuels*, 2013, **27**, 1391–1398.
- 583 45 D. C. Harris, *J. Chem. Educ.*, 1998, **75**, 119.
- 584 46 J. Yu, D. Plackett and L. X. L. Chen, *Polymer Degradation and Stability*, 2005, **89**, 289–299.
- 585 47 N. F. S. M. Farid, H. Ariffin, M. R. Z. Mamat, M. A. K. M. Zahari and M. A. Hassan, *RSC*  
586 *Adv.*, 2015, **5**, 33546–33553.
- 587 48 D. Pressman and H. J. Lucas, *J. Am. Chem. Soc.*, 1939, **61**, 2271–2277.
- 588 49 J. Benesty, J. Chen, Y. Huang and I. Cohen, in *Noise reduction in speech processing*, Springer,  
589 2009, pp. 1–4.
- 590 50 G. A. Hall, *J. Am. Chem. Soc.*, 1949, **71**, 2691–2693.
- 591 51 P. G. Maiella and T. B. Brill, *J. Phys. Chem.*, 1996, **100**, 14352–14355.
- 592 52 A. J. Belsky, P. G. Maiella and T. B. Brill, *J. Phys. Chem. A*, 1999, **103**, 4253–4260.
- 593 53 I. Lee, J. K. Cho and B.-S. Lee, *J. Chem. Soc., Perkin Trans. 2*, 1988, **0**, 1319–1323.
- 594 54 J. M. Clark, M. R. Nimlos and D. J. Robichaud, *J. Phys. Chem. A*, 2015, **119**, 501–516.

- 595 55 D. C. Elliott, B. Patrick, A. B. Ross, A. J. Schmidt and S. B. Jones, *Bioresource Technology*,  
596 2015, **178**, 147–156.
- 597 56 K.-D. Wendlandt, M. Jechorek, J. Helm and U. Stottmeister, *Journal of Biotechnology*, 2001,  
598 **86**, 127–133.
- 599 57 C. R. Fischer, A. A. Peterson and J. W. Tester, *Ind. Eng. Chem. Res.*, 2011, **50**, 4420–4424.
- 600 58 H. Pilath, A. Mittal, L. Moens, T. B. Vinzant, W. Wang and D. K. Johnson, in *Direct Microbial*  
601 *Conversion of Biomass to Advanced Biofuels*, ed. M. E. Himmel, Elsevier, Amsterdam, 2015,  
602 pp. 383–394.
- 603 59 S. M. Changi, J. L. Faeth, N. Mo and P. E. Savage, *Ind. Eng. Chem. Res.*, 2015, **54**, 11733–  
604 11758.
- 605 60 S. Kang and J. Yu, *RSC Adv.*, 2015, **5**, 30005–30013.
- 606 61 A. B. Ross, P. Biller, M. L. Kubacki, H. Li, A. Lea-Langton and J. M. Jones, *Fuel*, 2010, **89**,  
607 2234–2243.
- 608 62 L. Martino, M. V. Cruz, A. Scoma, F. Freitas, L. Bertin, M. Scandola and M. A. M. Reis,  
609 *International Journal of Biological Macromolecules*, 2014, **71**, 117–123.
- 610 63 G. N. Barnard and J. K. Sanders, *J. Biol. Chem.*, 1989, **264**, 3286–3291.
- 611 64 J. G. Linger, D. R. Vardon, M. T. Guarnieri, E. M. Karp, G. B. Hunsinger, M. A. Franden, C.  
612 W. Johnson, G. Chupka, T. J. Strathmann, P. T. Pienkos and G. T. Beckham, *PNAS*, 2014, **111**,  
613 12013–12018.
- 614 65 D. R. Vardon, S. B. K, J. Humberto, K. Dongwook, C. J. Kwon, C. P. N and S. T. J, *Green*  
615 *Chemistry*, 2014, **16**, 1507.
- 616 66 D. Kim, D. R. Vardon, D. Murali, B. K. Sharma and T. J. Strathmann, *ACS Sustainable Chem.*  
617 *Eng.*, 2016, **4**, 1775–1784.
- 618 67 G. W. Roberts, M.-O. P. Fortier, B. S. M. Sturm and S. M. Stagg-Williams, *Energy Fuels*,  
619 2013, **27**, 857–867.
- 620 68 J. Q. Bond, D. M. Alonso, D. Wang, R. M. West and J. A. Dumesic, *Science*, 2010, **327**, 1110–  
621 1114.
- 622 69 T. F. Degnan, C. M. Smith and C. R. Venkat, *Applied Catalysis A: General*, 2001, **221**, 283–  
623 294.
- 624 70 J. O. Metzger, *European Journal of Lipid Science and Technology*, 2009, **111**, 865–876.
- 625 71 IHS Markit, Chemical Economics Handbook (CEH) – Propylene,  
626 <https://ihsmarkit.com/products/propylene-chemical-economics-handbook.html>,  
627 (accessed December 6, 2018).
- 628 72 C. T. Nomura and S. Taguchi, *Appl Microbiol Biotechnol*, 2007, **73**, 969–979.
- 629 73 Z. A. Raza, S. Abid and I. M. Banat, *International Biodeterioration & Biodegradation*, 2018,  
630 **126**, 45–56.
- 631 74 J. Fu, X. Lu and P. E. Savage, *ChemSusChem*, 2011, **4**, 481–486.